JMEPEG (2011) 20:767–770
DOI: 10.1007/s11665-011-9916-1

©ASM International
1059-9495/$19.00

Effect of Ternary Addition of Iron on Shape Memory Characteristics of Cu-Al Alloys

T.N. Raju and V. Sampath

(*Submitted June 29, 2010; in revised form February 9, 2011*)

The effect of alloying Cu-Al alloys with Fe on their transformation temperatures and shape memory properties was investigated by differential scanning calorimetry and bend test. It was found that the minor additions of iron resulted in change of transformation temperatures and led to excellent shape memory properties of the alloys. Since the transformation temperatures are high, they are an ideal choice for high-temperature applications.

Keywords shape memory alloys, shape memory effect, transformation temperatures

1. Introduction

Shape memory alloys (SMAs) are a class of metallic materials that recover their original shape when subjected to an appropriate thermal or stress cycling. SMAs exhibit two phases: the low-temperature phase called martensite, and the high-temperature phase called austenite. The high-temperature phase is also referred to as the β (parent) phase. The phase transformations which occur between these two phases upon heating/cooling of martensite/austenite provide the basis for the unique properties of the SMAs. The two unique properties due to these solid phase transformations of martensite to austenite and austenite to martensite are the shape memory effect (SME) and superelasticity (SE). Shape memory alloys, such as those based on Ni-Ti, Cu, and Fe, have been found to be commercially attractive. Cu-based alloys are cheaper than Ni-Ti-based alloys, which are the most dominant among SMAs even today. They also exhibit better SME and SE than Fe-based alloys. Therefore, they attract greater attention for manifold engineering applications. However, the polycrystalline Cu-based SMAs, such as Cu-Al-Ni and Cu-Zn-Al, are too brittle and are, therefore, difficult to process them because of high degree of order and high elastic anisotropy of the parent phase (β) involved in it (Ref 1, 2).

Since SMAs are now considered as functional materials, there is an increasing need to develop SMAs with high transformation temperatures. At present, most of the SMAs have their transformation temperatures around room temperature. Applications such as automotive, robotics, power generation, and aerospace industries need SMAs that can operate at temperatures higher than 400 K. SMAs can be termed as high-temperature shape memory alloys (HTSMAs), if their austenitic start temperature remains above 390 K in stress-free conditions after any thermomechanical treatment (Ref 3).

In recent years, there have been intensive efforts to develop HTSMAs, and Ni-Ti-Zr, Ni-Ti-Hf, Ni-Ti-Pd, Ni-Al, and Ni-Mn SMAs are but a few worthy of mention. However, when it comes to application, they are not put to extensive use because of several problems. Among the HTSMAs, Ni-Ti-Zr and Ni-Al have poor workability, which makes it difficult to manipulate them into preferred shapes.

In Ni-Ti-Pd alloys, though good workability, high recovery strain and high martensitic transformation temperatures (up to 800 K) are achieved through suitable thermomechanical treatment, the high cost of Pd limits their potential applications. In the past few years, a new Cu-Al-Ag shape memory alloy with a high M_s transformation temperature ($M_s \geq 573$ K) has been developed. This serves as an impetus for the researchers to look for HTSMAs that are cheaper as well (Ref 3).

Cu-Al-Fe alloys like various other binary and ternary alloy systems undergo a martensitic transformation from the disordered β phase, which is usually stable at high temperatures. Upon quenching from the β-phase field, these alloys undergo a sequence of ordering reactions, $\beta \rightarrow \beta_2 \rightarrow \beta_1$ and subsequently form the ordered martensites α'_1, β'_1, γ'_1' depending on the amount of aluminum present in the alloys.

In this study, Cu-Al-Fe alloys were studied for their microstructures, transformation temperatures, and SME. This will prove to be beneficial for the application of the alloys as HTSMAs to function above 400 K with reasonably good SME.

2. Experimental Procedures

2.1 Alloy Preparation

Cu-Al-Fe alloys with 11-13 wt.% of aluminum and 0-5 wt.% of Fe were chosen for the present study. The composition of the alloys selected for the study exhibited

---

This article is an invited paper selected from presentations at Shape Memory and Superelastic Technologies 2010, held May 16-20, 2010, in Pacific Grove, California, and has been expanded from the original presentation.

T.N. Raju and **V. Sampath**, Department of Metallurgical and Materials Engineering, Indian Institute of Technology Madras, Chennai 600036, India. Contact e-mail: vsampath@iitm.ac.in.

β-phase and manifested SME on quenching to form martensite in this composition range. Pure copper, aluminum, and iron were taken in the right quantities, to make up a weight of 300 g of the alloy, and were melted together in an induction furnace under an argon atmosphere. The molten alloy was poured into a metallic mold of dimensions 150 mm × 100 mm × 3 mm, and allowed to solidify.

2.2 Thermomechanical Treatments

Thin strips of 100 mm × 20 mm × 3 mm were cut from the ingots. The strips were solution treated at 1173 K in the β-phase field for 6 h under an argon atmosphere and quenched into water at room temperature. The compositions of the alloys were determined using an atomic absorption spectrometer. Sheet specimens of 1 mm were obtained by hot rolling the cast alloy at 1073 K. All the rolled samples were solution treated at 1173 K for 15 min followed by step quenching them into a hot water bath at 373 K and subsequently quenching them into water at room temperature.

2.3 Characterization

The microstructures of the heat-treated specimens were examined by optical microscopy (OM). For transmission electron microscopy (TEM) studies, a small piece was cut from the rolled sample and mechanically polished on 1/0, 2/0, 3/0, 4/0 grade emery papers to reduce its thickness from 1 mm to 100 μm. A 3-mm disk was then cut out of the thinned sample using a disk cutter. The disk was thinned down by twin jet electropolishing on a Streurs-Tenupol jet polishing unit with a 30% HNO_3-70% methanol solution as the electrolyte at a temperature of −30 °C and a voltage of 12 V. The transmission electron microscopic (TEM) examination was performed on a Philips CM-20 electron microscope operating at 200 kV. The transformation temperatures were determined using a Perkins Elmer differential scanning calorimeter (DSC) from 323 to 773 K at a heating/cooling rate of 20 K/min. The phase analysis was carried out using a Brukers D8 x-ray diffractometer using Cu Kα radiation. The hot-rolled sheet specimens were subjected to bend test from 309 to 773 K for different pre-strains of 2, 3, 4, and 5% to determine shape memory recovery strain of the alloys by measuring the initial and final bend angles just before heating, i.e., when the sheet specimens were in the martensitic phase, and immediately after heating, i.e., when the specimens reverted to the austenitic phase of the alloys.

3. Results and Discussion

3.1 Microstructure and Transformation Temperatures

The chemical compositions and transformation temperatures of the alloys are tabulated in Table 1. The DSC curves for the step-quenched CAF1 and CAF2 alloys are shown in Fig. 1. The martensite to austenite transformation is endothermic, while the austenite to martensite transformation is exothermic. It can be observed in this alloy system that the martensite start (M_s) temperature, below which the alloy is completely martensitic, varies from 514 K to above 549 K. The martensite start (M_s) temperatures for Cu-Zn-Al, Cu-Al-Mn, and Cu-Al-Ni alloys are lower than 400 K compared to those for Cu-Al-Fe alloys. Therefore, these alloys can be designed to operate in this temperature range and can be treated as a potential alloy system for high-temperature applications.

Table 1 Chemical composition and transformation temperatures of Cu-Al-Fe alloys

Sample number	Composition, wt.%			Transformation temperature, K			
	Cu	Al	Fe	M_f	M_s	A_s	A_f
CA1	88.96	11.04	…	642	661	739	786
CA2	87.12	12.88	…	545	600	707	753
CAF1	87.61	11.45	0.94	505	521	715	751
CAF2	86.42	11.80	1.78	501	549	688	750
CAF3	85.03	12.08	2.89	498	531	686	748
CAF4	83.80	12.28	3.92	495	523	683	742
CAF5	82.75	12.52	4.73	482	514	654	715

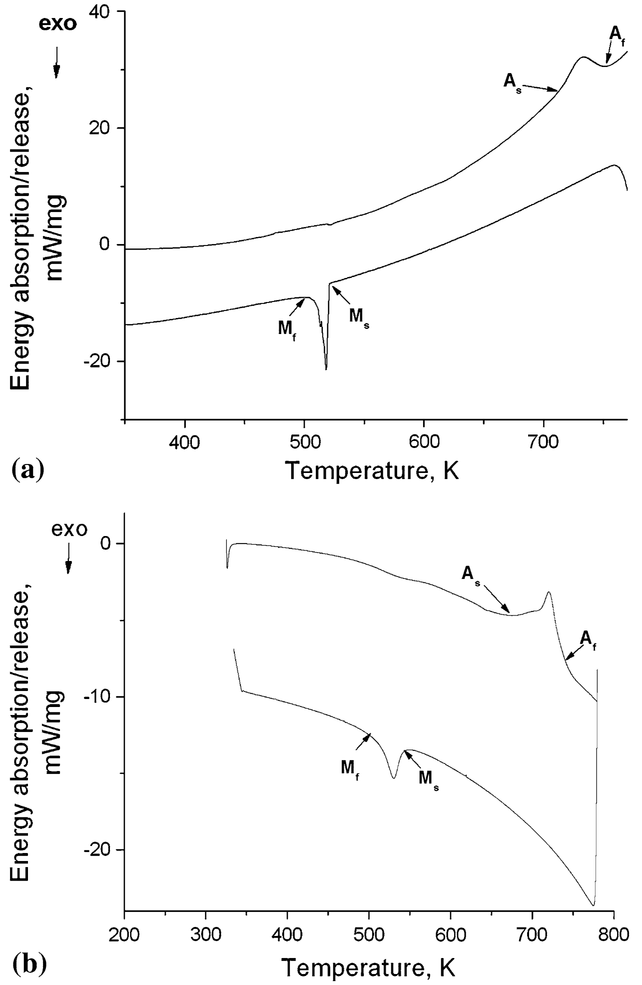

Fig. 1 DSC plots of (a) CAF1 and (b) CAF2 alloys

It is observed that, there is a variation of transformation temperatures due to variation in iron content. This is attributed to the formation of β_1' (18R) martensite at lower aluminum and iron contents. Table 1 shows how M_s and A_s vary as a function of the aluminum and iron contents of the alloys investigated. The transformation temperatures M_s and A_s decrease with an increase in the aluminum content. A similar effect is observed with the variation in iron content also.

The analysis of x-ray diffraction pattern was carried out to determine the presence of martensite using Cu Kα radiation. The x-ray diffraction patterns of the alloys at room temperature are shown in Fig. 2. By comparing the results obtained from the data in the JCPDS files with those published in the literature (Ref 4, 5), the peaks in the patterns were identified. It is observed that, in all the alloys, the major phase formed is β_1' martensite in varying amounts as indicated by the peak intensities.

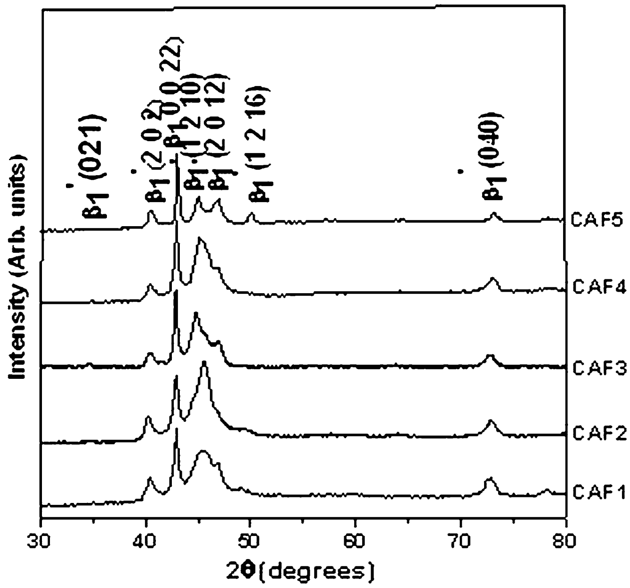

Fig. 2 X-ray diffraction patterns of Cu-Al-Fe alloys at room temperature

It is observed from Fig. 3(a) that CAF1 alloy shows predominantly β_1' type martensite, with much thicker martensitic plates, compared to other alloys, and has a fork-like morphology. This indicates complete transformation of austenite to martensite. The optical micrographs of alloys CAF2 (Fig. 3b), CAF3 (Fig. 3c), and CAF4 (Fig. 3d) show nucleation of martensitic plate groups (β_1') at a number of locations within the grains with different orientations and having plate-like morphology, but the plates are not as thin as those found in CAF1 alloy. The CAF5 alloy has martensitic plates with a similar morphology as in CAF4 alloy. Figure 4(a) shows the bright field TEM micrograph of the CAF1 alloy sample showing the β_1' martensite with characteristic zigzag plates indicated by arrows at the interface of two martensitic plates. It reveals the self-accommodating nature of the martensite. Owing to water quenching of the alloy samples, defects such as stacking faults, which are parallel to the basal plane are visible, as indicated by the arrows in Fig. 4(b) (Ref 6).

3.2 Shape Memory Effect (SME)

The strain recovery by SME of 1 mm thick hot-rolled specimens was determined by a semiempirical quantitative bend test (Ref 7-9). The-rolled sheet specimens of the alloys were subjected to different pre-strains of 2, 3, 4, and 5%. The rolled sheet specimens were bent around a mandrel to a U-shape in its martensitic phase, i.e., at a temperature below M_f (room temperature). The specimens were then heated to 773 K above their A_f temperature after being bent at room temperature. The corresponding angles of bend in their martensitic

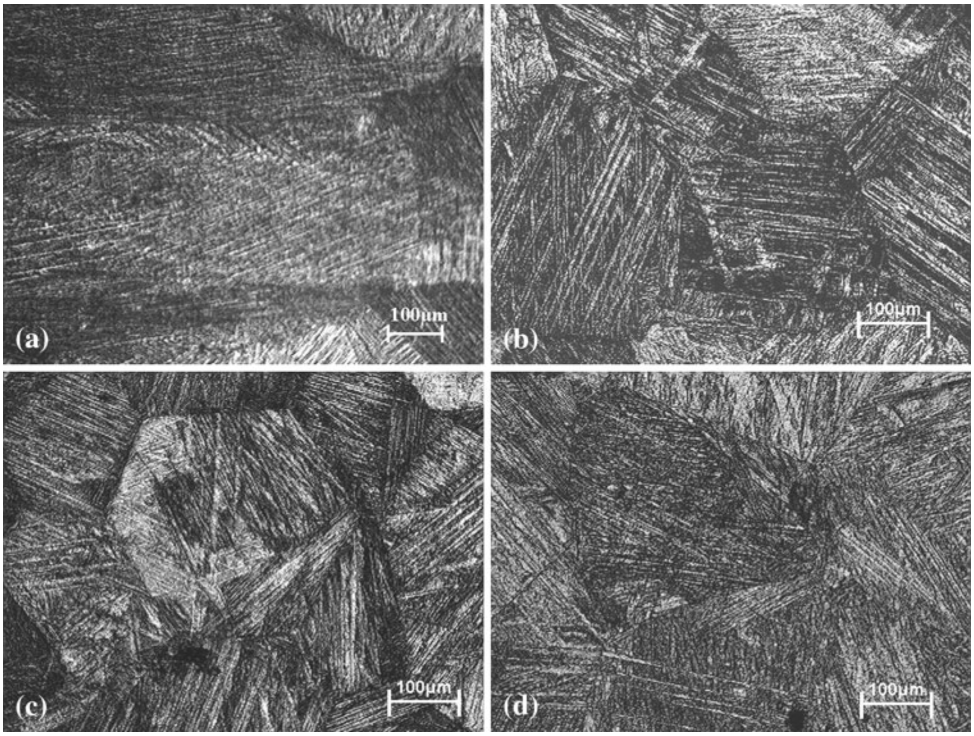

Fig. 3 Optical micrographs of Cu-Al-Fe alloys with different composition showing diverse martensitic variants: (a) CAF1; (b) CAF2; (c) CAF3; (d) CAF4

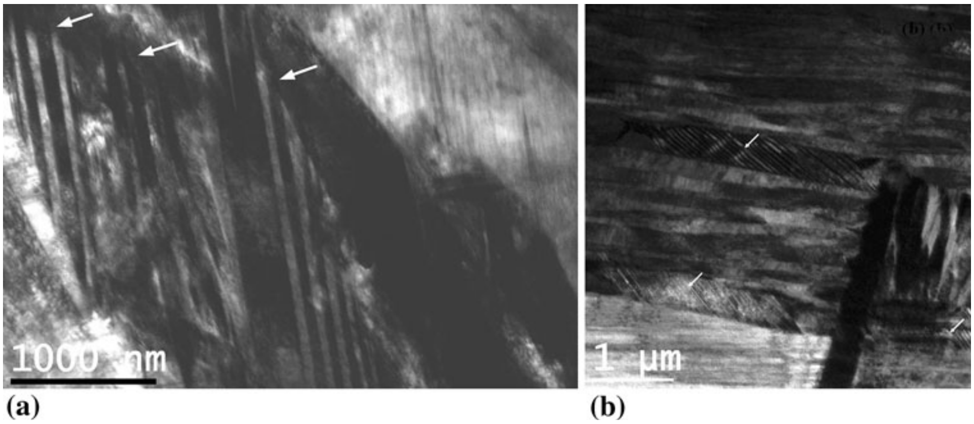

Fig. 4 TEM bright field images of CAF1 alloy showing: (a) zig-zag martensitic plates and (b) stacking faults introduced by water quenching

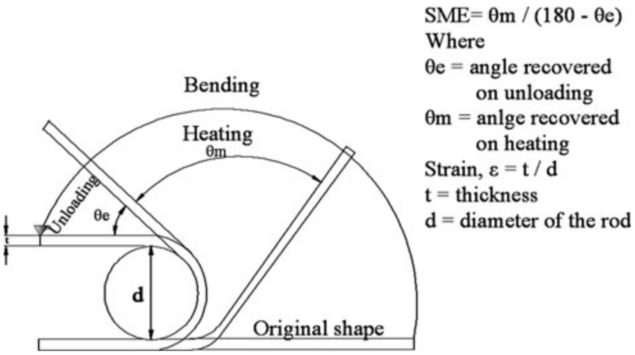

Fig. 5 Schematic diagram of bend test to determine strain recovery by SME

phase (i.e., before heating) and in its austenitic phase (i.e., after heating to above A_f temperature) as shown in Fig. 5 were measured and strain recovery by SME for different applied strains was determined. The amounts of strain recovery by SME by different alloys are given in Table 2.

It is observed from Fig. 2, that there is a variation in the intensity of martensitic peaks obtained from the alloy samples. The alloys CAF2 and CAF3 show higher intensity and correspondingly it is noted that these alloys exhibit better strain recovery by SME, when compared to alloys CAF1, CAF4, and CAF5. From this it is clear that the strain recovery by SME is proportional to the amount of martensitic phase present in different alloys. The alloys exhibit good strain recovery by SME, as much as 94-75% for applied pre-strains of 2-5%. It is observed that there is no significant variation in strain recovery due to change in the composition of the alloys.

Table 2 Strain recovery by SME by different alloys

	Strain recovery by SME, %			
Sample number	**2%**	**3%**	**4%**	**5%**
CAF1	85	82	88	80
CAF2	93	92	91	87
CAF3	92	91	91	94
CAF4	88	88	92	86
CAF5	86	84	84	75

4. Conclusions

(1) An increase in the aluminum and iron contents decreases the transformation temperatures, M_s and A_s. This indicates the dependence of transformation temperatures on chemical composition of the alloys.

(2) As the transformation temperatures of the alloys are higher compared with those of conventional SMAs, they can be suitably designed to function in high-temperature applications.

(3) The alloys do not show any significant variation in strain recovery by SME because of variation in composition of the alloys.

References

1. K. Otsuka and C.M. Wayman, *Shape Memory Materials*, 1st ed., Cambridge University Press, Cambridge, UK, 1998, p 97
2. E. Hombogen and N. Jost, *The Martensitic Transformation in Science and Technology*, Butterworth-Heinemann, London, 1990, p 15
3. G.S. Fristov, J. Van Humbeeck, and Yu.N. Koval, High Temperature Shape Memory Alloys-Problems and Prospects, *J. Intell. Mater. Syst. Struct.*, 2006, **17**, p 1041–1047
4. J.M. Vanderberg and C.W. Draper, An X-Ray Diffraction Study on the Microstructure of Laser Surface Melted Cu-Al-Fe Alloys, *Mater. Lett.*, 1984, **2**, p 386–392
5. W.S. Li, Z.P. Wang, Y. Lu, Y.U. Jin, L.H. Yuan, and F. Wang, Mechanical and Tribological Properties of a Novel Aluminium Bronze Materials for Drawing Dies, *Wear*, 2006, **261**, p 155–163
6. J.M. Guilemany, E. Peregrin, F.C. Lovey, N. Llorca, and E. Cesari, TEM Study of β and Martensite in Cu-Al-Mn Shape Memory Alloys, *Mater. Charact.*, 1991, **26**, p 23–28
7. C.M. Wayman, The Shape Memory Effect, *Met. Forum*, 1981, **4**, p 135–141
8. R. Kainuma, S. Takahashi, and K. Ishida, Thermoelastic Martensite and Shape Memory Effect in Ductile Cu-Al-Mn Alloys, *Met. Trans. A*, 1996, **27A**, p 2187–2195
9. U.S. Mallik and V. Sampath, Effect of Alloying on Microstructure and Shape Memory Characteristics of Cu-Al-Mn Shape Memory Alloys, *Mater. Sci. Eng. A*, 2008, **481–482**, p 680–683